

# Can we analyze the Ni K edge EXAFS near the Gd L<sub>1</sub> edge in a metallic compound GdNi<sub>2</sub>?

Ikuo NAKAI<sup>a</sup>, Isuke OUCHI<sup>a</sup> and Hironobu MAEDA<sup>b</sup>

(Accepted 21 June 1994)

## Abstract

Extended X-ray absorption fine structure (EXAFS) measurements have been carried out for the Ni K edge of a metallic compound GdNi<sub>2</sub>, which stands near the Gd L<sub>1</sub> edge. We investigate whether the analysis for the Ni K edge gives useful information on the local structure around a central Ni atom. The interatomic distance thus obtained is almost the same value as the crystallographic distance determined from X-ray diffraction measurements: 2.53 Å and 2.97 Å for the nearest neighbor Ni-Ni and Ni-Gd interatomic distance.

## 1. Introduction

Extended X-ray absorption fine structure (EXAFS) has received much attention as a powerful method for studying the local atomic structure around a specific absorbing atom.<sup>(1)–(5)</sup> A typical tool for the structure analysis is the X-ray diffraction. It is based on a long-range periodic structure of component atoms. Therefore it is completely useless for materials without the long-range periodic structure such as gases, liquids and amorphous solids. On the other hand, EXAFS analysis needs not the periodicity of the component atoms and is quite a useful method for such materials.

From a precise investigation of the temperature dependence of the magnetization we have found that the spin wave stiffness constant connects closely with the paramagnetic Curie temperature in an amorphous ferromagnet Gd<sub>67</sub>Ni<sub>33</sub><sup>(6)</sup> as well as an amorphous system Gd<sub>x</sub>Y<sub>68-x</sub>Cu<sub>32</sub>.<sup>(7)–(9)</sup> The amorphous Gd<sub>67</sub>Ni<sub>33</sub> system is regarded as a typical nearest neighbor Heisenberg ferromagnet with fluctuations in the exchange interaction. This means that the magnetic behavior of the system relates to structural

---

<sup>a</sup>Department of Physics, Faculty of General Education, Tottori University, Tottori 680

<sup>b</sup>Department of Chemistry, Faculty of Science, Okayama University, Okayama 700

parameters such as the coordination number, the interatomic distance and the mean square relative displacement. Therefore the structural parameter is a key to investigate the relation between magnetism and structure for such amorphous materials.

We have measured EXAFS for the amorphous ferromagnet  $\text{Gd}_{67}\text{Ni}_{33}$  around a Gd atom and obtained the structural parameters around the Gd component.<sup>10,11</sup> An EXAFS spectrum for a Ni K edge of the ferromagnet inevitably contains a signal of the Gd  $L_1$  edge because the Ni K edge (8.339 keV) is very close to the Gd  $L_1$  edge (8.376 keV). Usually one may consider that it is completely impossible to analyze EXAFS for the Ni K edge and to obtain information on surroundings of Ni atoms. However, we have an advantage that the EXAFS signal of the Gd  $L_1$  edge is much weaker than that of the Ni K edge. Therefore there may be a little possibility of our analyzing the EXAFS signal about the Ni K edge for the amorphous  $\text{Gd}_{67}\text{Ni}_{33}$  ferromagnet. To make sure whether there is the possibility or not, we attempt to measure and to analyze the Ni K edge EXAFS of a metallic compound  $\text{GdNi}_2$  which has been already identified to have a  $\text{MgCu}_2$ -type C15 Laves phase structure with a lattice constant of  $7.2056 \pm 0.0009 \text{ \AA}$ .<sup>12</sup>

## 2. Experimental Details

The metallic compound  $\text{GdNi}_2$  was prepared from 3N Gd and 4N Ni by arc melting in an argon atmosphere. The ingot was ground into a fine powder of less than  $20 \mu\text{m}$  in diameter. The powder was stuck uniformly on an adhesive tape. A specimen for the measurement was a few pieces of tapes piled up. We prepared specimens of a crystalline Gd powder and a Ni thin film of  $5 \mu\text{m}$  thick as references.

Measurements were carried out at the beam line 6B of the Photon Factory (PF), the National Laboratory for High Energy Physics (KEK) in Tsukuba.<sup>13</sup> The storage ring of the synchrotron radiation was operated with a positron energy of 2.5 GeV and a current of 350 mA in maximum. A Si (111) double-crystal monochromator was set up in the beam line 6B. The beam from the storage ring contained higher harmonics, which did a serious damage to the EXAFS data. To eliminate the higher harmonics from the beam, we inclined two crystals of the monochromator from the parallel form by a few seconds. This detuning of the crystals reduced the strength of the beam incident on the specimen from the maximum to 60%. The EXAFS spectrum was measured at 300 K in a transmission mode. Intensities of photons incident upon the specimen and passed through it,  $I_0$  and  $I$ , were detected with two independent ionization chambers: one was of 17 cm in length filled with a nitrogen gas flowing and the other was of

31 cm with a mixed gas of 85% nitrogen and 15% argon. The energy of photons was corrected with the energy value for a peak near the Cu K edge (8.9788 keV).

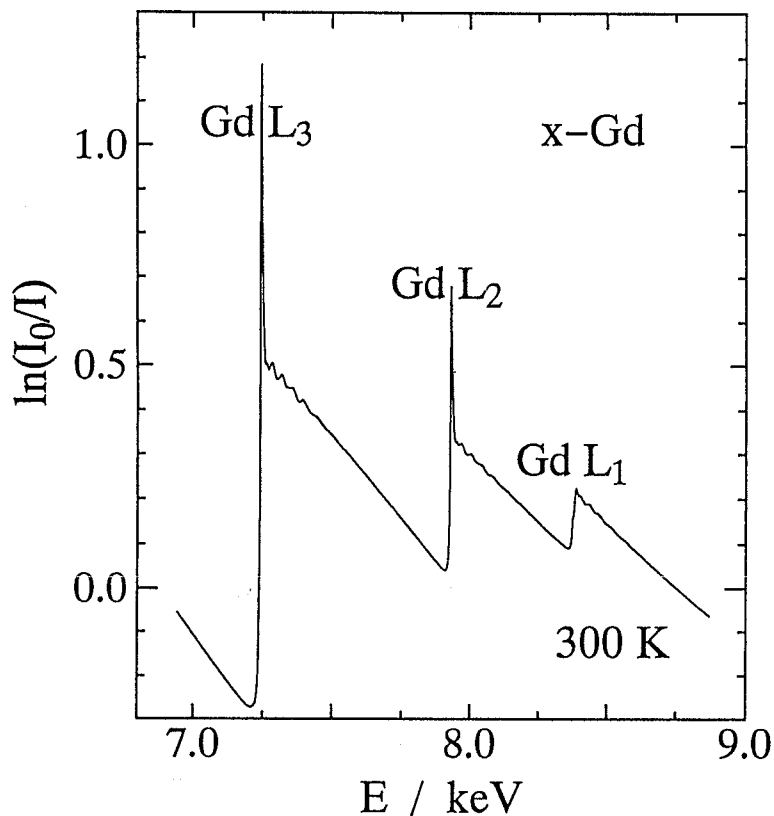


Fig.1 Observed total absorption  $\ln(I_0/I)$  around Gd L<sub>3</sub>, L<sub>2</sub> and L<sub>1</sub> edges as a function of photon energy  $E$  for a crystalline Gd metal at 300 K.

### 3. Results

Figure 1 shows the total X-ray absorption  $\ln(I_0/I)$  as a function of photon energy  $E$  about L edges for the Gd powder specimen. The EXAFS oscillation is appeared in higher energy range than each edge or L<sub>3</sub>, L<sub>2</sub> and L<sub>1</sub>. A remarkably sharp absorption at the L<sub>3</sub> and L<sub>2</sub> edges, which is called a *white line*, is a common feature for the L<sub>3</sub> and L<sub>2</sub> edges of rare-earth atoms; on the other hand, the *white line* is not observed at the L<sub>1</sub> edge. The total absorption for the Ni K edge of the crystalline Ni thin film is shown

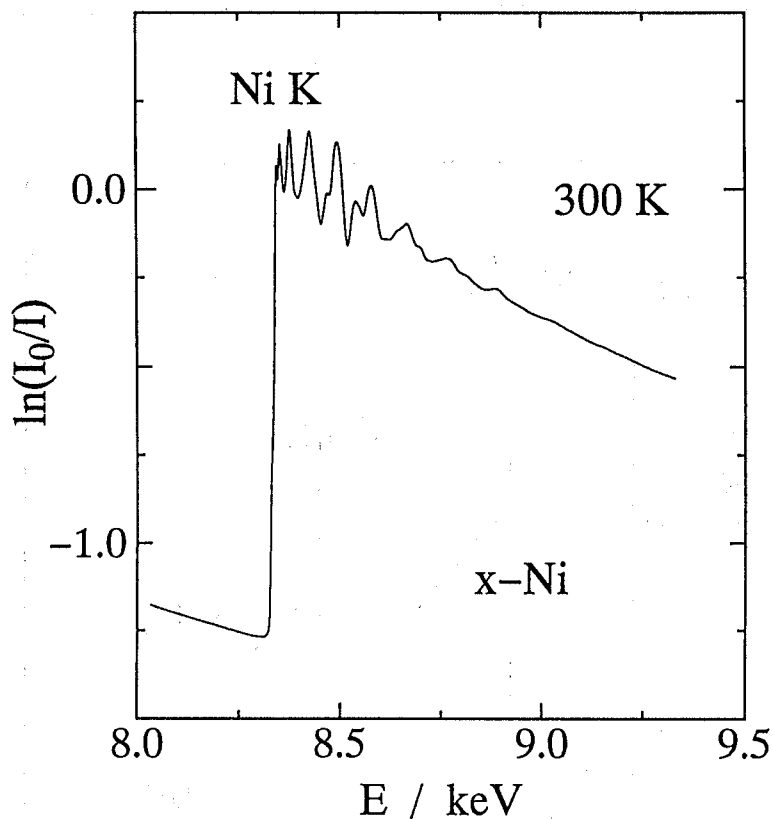


Fig.2 Observed total absorption  $\ln(I_0/I)$  around a Ni K edge versus photon energy  $E$  for a crystalline Ni metal at 300 K.

in Fig.2. The absorption for the  $\text{GdNi}_2$  metallic compound is illustrated in Fig.3. The arrows represent the energy values at the Ni K and Gd  $L_1$  edges. The sudden change in absorption and the subsequent small peak between the arrows comes from the Ni K edge; on the other hand, the rather slow increase in higher energy region than the peak is due to the Gd  $L_1$  edge. The overlap of the EXAFS signals above the Ni K and Gd  $L_1$  edges puts us at a serious disadvantage when we analyze EXAFS for the Ni K edge. As seen in Fig.1, the following features are about the Gd  $L_1$  edge: the jump of the absorption is quite small without the *white line* and the EXAFS signal is also weak. These may help us to derive useful information on the local structure around the Ni atom from the EXAFS signal above the Ni K edge.

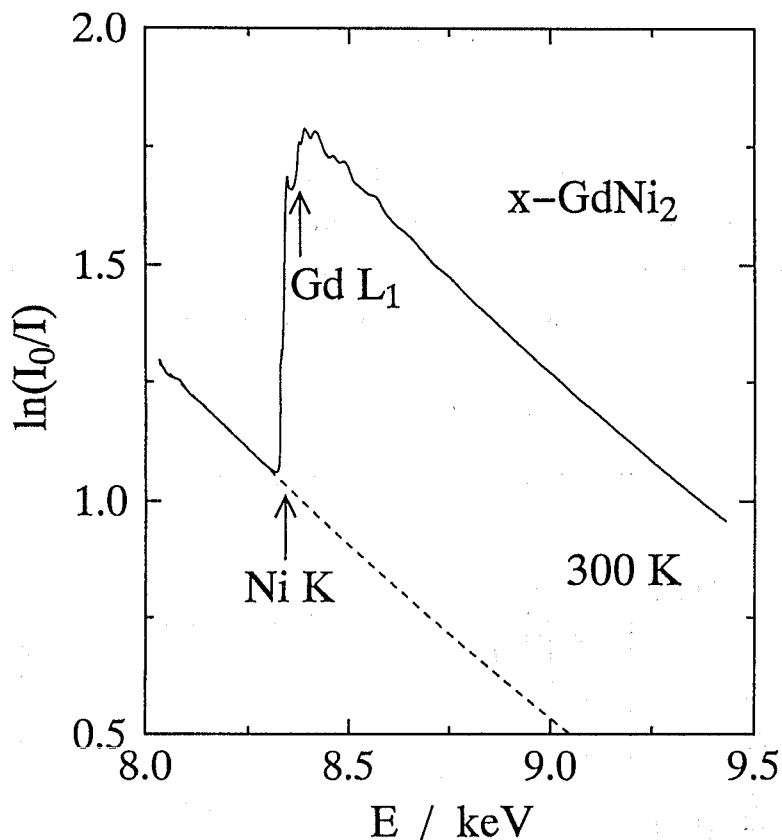


Fig.3 Observed total absorption  $\ln(I_0/I)$  around Ni K and Gd L<sub>1</sub> edges plotted against photon energy  $E$  for a metallic compound GdNi<sub>2</sub> at 300 K. The arrow indicates a threshold energy for each edge.

#### 4. Analysis and Discussion

The following routine steps of procedure will be applied in analyzing the observed absorption around the Ni K edge of the metallic compound GdNi<sub>2</sub> in Fig.3: the first step is to derive a Fourier filtered EXAFS spectrum from the absorption; the second is to fit the spectrum to a theoretical EXAFS formula and to determine the structural parameters.<sup>10</sup>

The X-ray absorption coefficient  $\mu_a$  means the total X-ray absorption divided by the thickness of the specimen  $d$ , which is given by

$$\begin{aligned}\mu_d &= \ln(I_0/I)/d \\ &= \mu_v + \mu,\end{aligned}\quad (1)$$

where  $\mu_v$  is the background contribution due to all the atoms but the specific absorbing atom to be questioned, which is estimated from the best fit of the absorption in lower energy region than the Ni K edge to a Victoreen formula  $\mu_v = A/E^3 + B/E^4 + C$  as shown by the dotted line in Fig.3. The solid line in Fig.4 denotes  $\mu d$ . The EXAFS signal  $\chi(k)$  is derived from  $\mu$  as follows

$$\chi(k) = (\mu - \mu_s) / \mu_s, \quad (2)$$

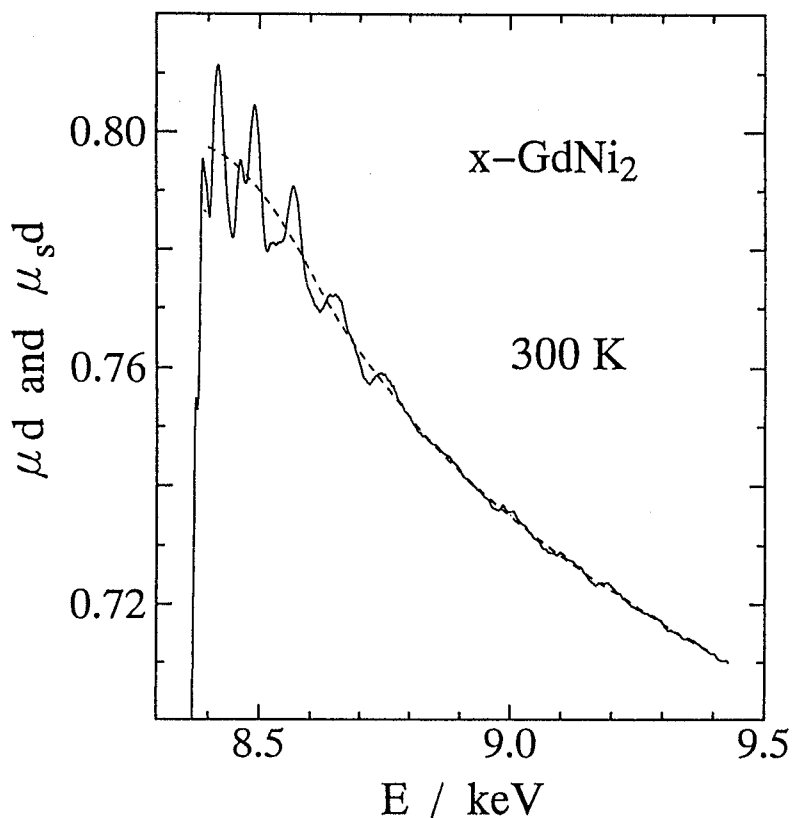


Fig.4 Absorption  $\mu d$  or the difference between the total absorption and the background, where  $d$  is the thickness of the specimen, as a function of photon energy  $E$  for a metallic  $\text{GdNi}_2$  compound at 300 K. The broken line denotes a hypothetical absorption  $\mu_s d$  for an isolated atom estimated from the cubic spline technique.

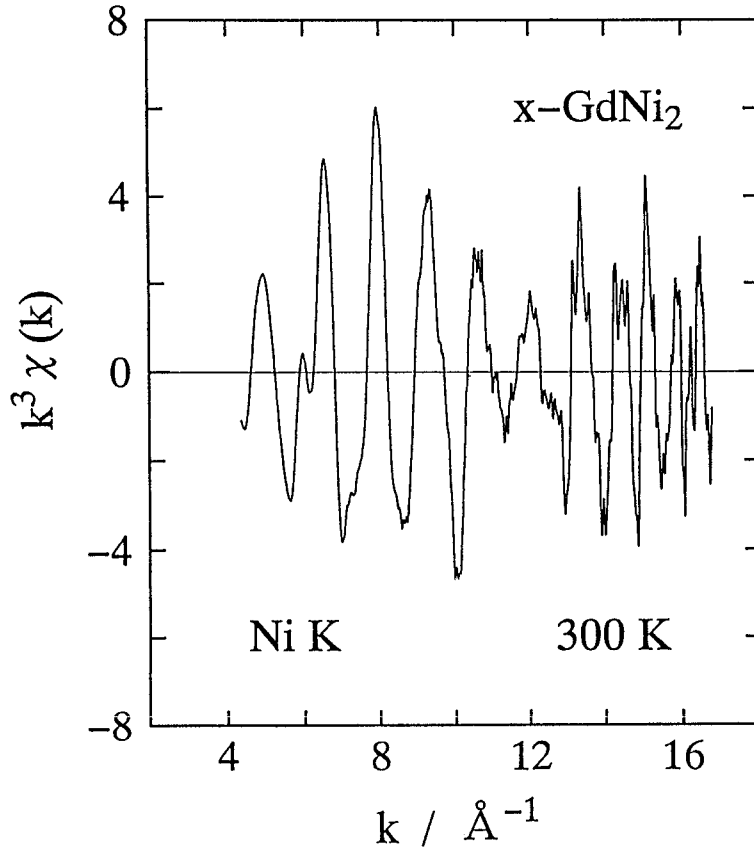


Fig.5 EXAFS spectrum  $k^3 \chi(k)$  versus wave vector  $k$  for the Ni K edge of a metallic compound GdNi<sub>2</sub> at 300 K.

where  $\mu_{sd}$  means a hypothetical absorption when the central atom in question is isolated from the other atoms. It is evaluated from the cubic spline technique and is drawn by the dotted line in Fig.4. The photoelectron wave vector  $k$  is represented by  $k = [2m(E - E_0)/\hbar^2]^{1/2}$  when  $m$  is the mass of an electron and  $E_0$  is the threshold energy of an edge. In the first step of analysis  $E_0$  is assumed to be the photon energy at the first inflection point of the edge. As seen in Fig.4, the more the energy increases, the less the amplitude of  $\chi(k)$  becomes. To emphasize  $\chi(k)$  in the higher energy region, we derive an EXAFS spectrum  $k^3 \chi(k)$  as shown in Fig.5. In the figure we cannot find an explicit influence of the Gd L<sub>1</sub> signal for  $k$  range more than  $4.36 \text{ \AA}^{-1}$ , which corresponds to 8.40 keV. However, we should keep our mind on a possibility of including a little effect of the Gd L<sub>1</sub> signal in  $k^3 \chi(k)$  of Fig.5. Fourier transformation of  $k^3 \chi(k)$  makes a radial structure function  $\Phi(R)$

$$\Phi(R) = \frac{1}{\sqrt{2\pi}} \int_{k_{\min}}^{k_{\max}} W(k) k^3 \chi(k) \exp[-2ikR] dk$$

$$= \text{Re}[\Phi(R)] + i\text{Im}[\Phi(R)]. \quad (3)$$

The influence of restricting the Fourier transform between  $k_{\min}=4.36 \text{ \AA}^{-1}$  and  $k_{\max}=12.97 \text{ \AA}^{-1}$  is reduced by the Hanning window function  $W(k)$ . We choose the rather large value of  $4.36 \text{ \AA}^{-1}$  as  $k_{\min}$ , which corresponds to the energy higher by about 60 eV than the Ni K edge and by about 25 eV than the Gd L<sub>1</sub> edge, to make the influence of the Gd L<sub>1</sub> signal on the Ni K edge EXAFS as small as possible. Figure 6 shows the imaginary part (thick line) and the absolute value (thin line) of  $\Phi(R)$  for the Ni K

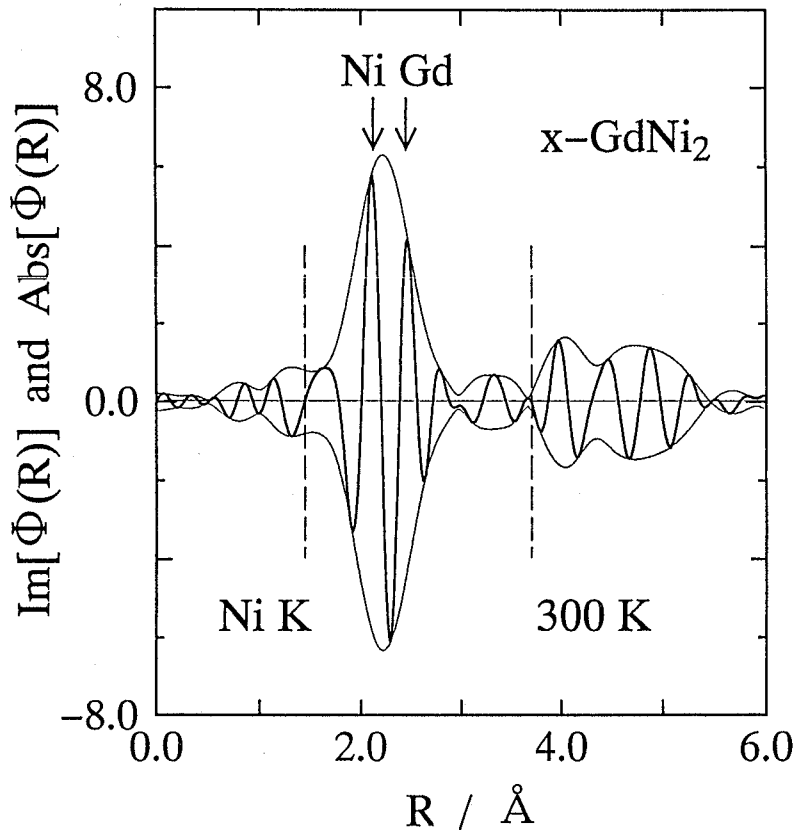


Fig.6 Imaginary part  $\text{Im}[\Phi(R)]$  (thick line) and absolute  $\text{Abs}[\Phi(R)]$  (thin line) of the radial structure function  $\Phi(R)$  for a metallic  $\text{GdNi}_2$  compound at 300 K. The distance  $R$  from a central Ni atom is not corrected for phase shifts. Peak positions of the imaginary part (arrows) correspond to distances of the nearest Ni and Gd neighbors.



edge of GdNi<sub>2</sub>. The absolute value  $\text{Abs}[\Phi(R)]$  is given by  $\{(\text{Re}[\Phi(R)])^2 + (\text{Im}[\Phi(R)])^2\}^{1/2}$  where  $\text{Re}[\Phi(R)]$  and  $\text{Im}[\Phi(R)]$  mean the real and imaginary part of  $\Phi(R)$ . The two peaks for  $\text{Im}[\Phi(R)]$  shown by the arrows correspond to the positions of the nearest neighbor Ni and Gd atoms around the central Ni component. It should be emphasized that  $R$  is not corrected for the phase shift; therefore the positions of the peaks, 2.11 Å and 2.46 Å, are a little smaller than the distances evaluated from the non-linear least squares fit in the second step of analysis. To obtain the Fourier filtered EXAFS spectrum, we transform  $\Phi(R)$  into  $k^3\chi(k)$  again by using the Fourier filtering technique which selects only a useful piece of information on a neighboring atom to be questioned. Since the nearest neighbor Ni and Gd atoms are of great interest at the present work, the Fourier transformation is applied for the  $R$  range between 1.43 Å and 3.70 Å as shown by a couple of broken lines in the figure. The Fourier filtered EXAFS spectrum  $k^3\chi(k)$  thus obtained is shown by the open circle in Fig.7.

Paying much attention to the fact that the spectrum may include the influence of the Gd L<sub>1</sub> edge, we make the next step of analysis, that is, the non-linear least squares fitting of the Fourier filtered  $k^3\chi(k)$  spectrum for the theoretical EXAFS equation<sup>(3)-(5)</sup>

$$k^3\chi(k) = \sum_j A_j(k) \sin [2kR_j + \delta_j(k)], \quad (4)$$

where the amplitude is given as

$$A_j(k) = \frac{N_j k^2}{R_j^2} F_j(k) S(k) \times \exp[-2\sigma_j^2 k^2] \exp[-2R_j/\lambda_j(k)]. \quad (5)$$

Here  $R_j$  is the distance between the central absorbing atom and the  $j$ -th neighbor,  $\delta_j(k)$  is the phase shift,  $N_j$  is the coordination number,  $\sigma_j^2$  is the mean square relative displacement or the Debye-Waller factor which consists of thermal vibration and static disorder,  $F_j(k)$  is the backscattering amplitude and  $S(k)$  is the amplitude reduction factor. The electron mean free path  $\lambda_j(k)$  is given by  $\lambda_j(k) = k/\eta$  with a parameter  $\eta$ . In the present work we use theoretical values by McKale et al for  $\delta_j(k)$  and  $F_j(k)$ .<sup>16</sup>

To obtain the local structure around the Ni atom, we carry out the non-linear least squares fitting of the Fourier filtered  $k^3\chi(k)$  spectrum in Fig.7 for eqs.(4) and (5). A structural model with two shells is used because the spectrum contains information on the nearest Ni and Gd neighbors around the central Ni atom. The metallic compound GdNi<sub>2</sub> shows the MgCu<sub>2</sub>-type C15 Laves phase with the lattice

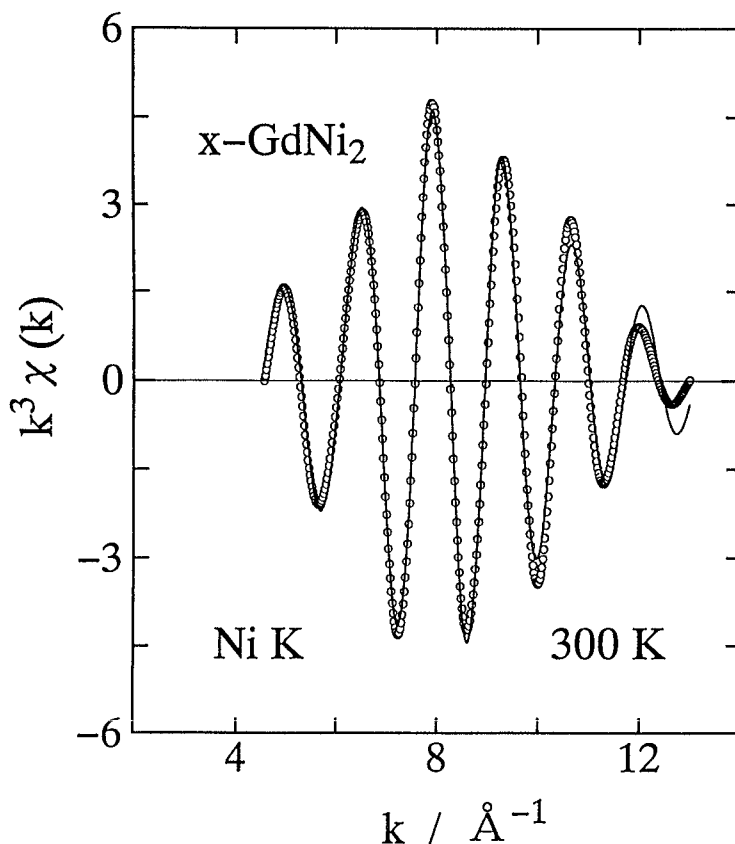


Fig.7 Fourier filtered EXAFS spectrum  $k^3\chi(k)$  (circle) and the best fit (solid line) for the Ni K edge of a metallic compound  $\text{GdNi}_2$  at 300 K.

constant of  $7.2056 \pm 0.0009 \text{ \AA}$  determined from X-ray diffraction as mentioned in section 1.<sup>12</sup> From the lattice constant the nearest neighbor Ni-Ni and Ni-Gd distances are estimated to be  $2.5476 \text{ \AA}$  and  $2.9873 \text{ \AA}$  respectively. In the C15 Laves phase 6 Ni and 12 Gd atoms surround the central Ni atom. Taking these as the initial values for the structural parameters, we start on the best fit for the Fourier filtered EXAFS spectrum  $k^3\chi(k)$  shown in Fig.7. In the fit the coordination numbers are fixed to be 6 for the Ni shell and 12 for the Gd shell; therefore the disposable parameters are the distance, the mean square relative displacement, the electron mean free path, and the difference between the threshold of the edge assumed in the first step of analysis and the true energy estimated in the second step. In the fitting process the threshold energy and the wave vector are corrected for the difference. The structural parameters thus determined are listed in Table 1. The solid line in Fig.7 shows  $k^3\chi(k)$  calculated from

**Table 1** Structural parameters determined from the non-linear least squares fit of the EXAFS analysis for the metallic compound GdNi<sub>2</sub>: the coordination number  $N$ , the interatomic distance  $R$ , the mean square relative displacement  $\sigma^2$ , the threshold energy  $E_0$  and the parameter  $\eta$  related to the electron mean free path. The numbers in parentheses denote the statistical uncertainties.

A - B <sup>a)</sup>	$E_0/\text{keV}$	$N^{\text{b)}$	$R_{\text{cal}}/\text{\AA}^{\text{b)}$	$R/\text{\AA}$	$\sigma^2/\text{\AA}^2$	$\eta/\text{\AA}^{-2}$
Ni-Ni	8.339	6	2.5476	2.53(1)	0.011(1)	1.45(7)
Ni-Gd		12	2.9873	2.97(1)	0.030(2)	1.45(7)
Gd-Ni	7.249 <sup>c)</sup>	12	2.9873	2.97(2) <sup>c)</sup>	0.022(2) <sup>c)</sup>	
Gd-Gd		4	3.1201	3.17(1) <sup>c)</sup>	0.013(1) <sup>c)</sup>	

a) A is a central absorbing atom and B is a backscattering neighbor.

b) The crystallographic values for a MgCu<sub>2</sub>-type C15 Laves phase structure with a lattice constant of  $7.2056 \pm 0.0009 \text{ \AA}$ .<sup>(12)</sup>

c) The values are quoted from ref. (10).

the theoretical EXAFS formulae, eqs. (4) and (5), with these values for the parameters, which agrees well with the Fourier filtered EXAFS spectrum  $k^3\chi(k)$  shown by the circle.

If the fit gave unreasonable values for the parameters, we would have to conclude the failure of EXAFS analysis for the Ni K edge. Fortunately, however, we have obtained reasonable results for the parameters as follows: the nearest neighbor Ni-Ni and Ni-Gd atomic distances, 2.53 Å and 2.97 Å, are nearly equal to the crystallographic values mentioned above; the Ni-Gd distance in the present work is in good agreement with the Gd-Ni distance determined from analysis for a Gd L<sub>3</sub> edge previously.<sup>10</sup> These results confirm the validity of the present analysis for the Ni K edge. Therefore we come to the conclusion that we can analyze the Ni K edge EXAFS near the Gd L<sub>1</sub> edge and obtain useful information on the local structure around the Ni atom for the metallic compound GdNi<sub>2</sub>. This conclusion may be extended for another Gd-Ni alloys such as the amorphous Gd<sub>67</sub>Ni<sub>33</sub> ferromagnet.

## 5. Conclusions

We have measured and analyzed the Ni K edge EXAFS near the Gd L<sub>1</sub> edge to test whether we get useful information on the local structure around the central Ni atom. The EXAFS spectrum about the Ni K edge includes a weak Gd L<sub>1</sub> signal. However, the analysis gives a reasonable result for the local structure around the Ni atom, if we minimize the effect of the Gd L<sub>1</sub> signal by choosing a rather high  $k_{\text{min}}$  value in the Fourier transformation and then analyze them carefully keeping our mind on the possibility of influence of the Gd L<sub>1</sub> edge.

### Acknowledgments

We wish to thank Professor Yoshikazu Andoh at Faculty of Education, Tottori University for his help in preparation of the metallic compound GdNi<sub>2</sub>. The measurement was performed under the approval of the PF Program Advisory Committee (Proposal No. 92020).

### References

- (1) D. E. Sayers, E. A. Stern and F. W. Lytle: Phys. Rev. Lett. **27**(1971)1204.
- (2) F. W. Lytle, D. E. Sayers and E. A. Stern: Phys. Rev. **B11**(1975)4825.
- (3) E. A. Stern: Phys. Rev. **B10**(1974)3027.
- (4) C. A. Ashley and S. Doniach: Phys. Rev. **B11**(1975)1279.
- (5) P. A. Lee and J. B. Pendry: Phys. Rev. **B11**(1975)2795.
- (6) I. Nakai and T. Fukagawa: J. Phys. Soc. Jpn. **62**(1993)2456.
- (7) I. Nakai, C. A. Cornelius, S. H. Kilcoyne, E. W. Lee and B. D. Rainford: J. Phys. Soc. Jpn. **57**(1988)2506.
- (8) I. Nakai: *Proc. 2nd Int. Symp. on Physics of Magnetic Materials, Beijing, 1992* (International Academic Publishers, Beijing, 1992) Vol. 1, p. 172.
- (9) I. Nakai, H. Maeda and A. Ishii: *Physics of Transition Metals*, ed. P. M. Oppeneer and J. Kübler (World Scientific, Singapore, 1993) Vol. 2, p. 954.
- (10) I. Nakai: J. the Faculty of General Education, Tottori University **25**(1991)95.
- (11) I. Nakai and H. Maeda: Jpn. J. Appl. Phys. **32**(1993)Suppl. 32-2 685.
- (12) N. C. Baenziger and J. L. Moriarty, Jr. : Acta Cryst. **14**(1961)948.
- (13) M. Nomura and A. Koyama: *Users' Manual of BL6B and 7C at Photon Factory*, KEK Internal 93-1(1993), National Laboratory for High Energy Physics.
- (14) H. Maeda: J. Phys. Soc. Jpn. **56**(1987)2777.
- (15) A. D. McKale, B. W. Veal, A. P. Paulikas, C. -K. Chan and G. S. Knapp: J. Am. Chem. Soc. **110**(1988)3764.